Single Nodal Loop of Accidental Degeneracies in Minimal Symmetry: Triclinic CaAs_{3}

Y. Quan, Z. P. Yin, and W. E. Pickett

Phys. Rev. Lett. **118**, 176402 — Published 25 April 2017

DOI: 10.1103/PhysRevLett.118.176402

A single nodal loop of accidental degeneracies in minimal symmetry: triclinic $CaAs_3$

Y. Quan and Z. P. Yin
Department of Physics and Center for Advanced Quantum Studies, Beijing Normal University, Beijing 100875, China

W. E. Pickett
Department of Physics, University of California Davis, Davis CA 95616

(Dated: March 6, 2017)

The existence of closed loops of degeneracies in crystals has been intimately connected to associated crystal symmetries, raising the question: what is the minimum symmetry required for topological character, and can one find an example? Triclinic $CaAs_3$, in space group $P\bar{1}$ with only a center of inversion, has been found to display, without need for tuning, a nodal loop of accidental degeneracies with topological character, centered on one face of the Brillouin zone that is otherwise fully gapped. The small loop is very flat in energy, yet is cut four times by the Fermi energy, a condition that results in an intricate repeated touching of inversion related pairs of Fermi surfaces at Weyl points. Spin-orbit coupling lifts the fourfold degeneracy along the loop, leaving trivial Kramers pairs. With its single nodal loop that emerges without protection from any point group symmetry, $CaAs_3$ represents the primal "hydrogen atom" of nodal loop systems.

Nodal loop semimetals (NLSs) represent the most delicate type of topological phase in the sense that they arise from a closed loop of *accidental* degeneracies in the Brillouin zone. In some ways they complement the topological character of Weyl semimetals[1] by displaying surface Fermi arcs or Fermi lines, or both. Several structural classes of NLSs have been identified, always associated with specific space group symmetries that enable, or in common parlance protect, the necessary degeneracies. On the other hand, the early theoretical work[2,3] presumed only the minimum symmetry necessary to allow a nodal loop: time reversal symmetry and a center of inversion. This limiting case of "minimal symmetry" has prompted us to look for an example and understand its behavior.

When the little group at wavevector $\vec{k}$ contains only the identity, the Hamiltonian $H(\vec{k})$ has matrix elements between states with neighboring eigenvalues and anticrossings occur as some parameter of H is varied. von Neumann and Wigner first investigated the conditions under which degeneracies nevertheless occur, so-called accidental degeneracies,[4] where matrix elements vanish for no physical reason. Herring generalized their arguments to accidental degeneracies in three dimensional (3D) crystals.[2,3] with some extension by Blount.[5] Herring pointed out, for example, that a mirror plane provides a natural platform for a ring of degeneracies. If a band with even mirror symmetry is higher in energy than a band of odd symmetry at $\vec{k}_1$ but lower at $\vec{k}_2$ (both on the mirror plane), then due to the continuity of eigenvalues and differing symmetry, on any path connecting them there must be a point of degeneracy. The locus of such degeneracies maps out either a loop encircling one of the points, or an extended line from zone to zone separating the two points (which, considering periodicity, also becomes a closed loop topologically).

The topologically singular nature of such nodal loops was established by Berry.[6] Allen demonstrated[7] how, with minimal symmetry available, these loops of degeneracies are destroyed by spin-orbit coupling (SOC). Special symmetries can enable nodal loops in the presence of SOC, for example a screw axis in the example of Fang *et al.*[8] Burkov *et al.* made the modern rediscovery of nodal loops and illustrated the type of Weyl-point connected electron and hole Fermi surface that should be expected when the band energies around the loop cross the Fermi energy.[9] Such nodal loops should be common, and indeed have been found even in high symmetry elemental metals.[10] Nodal loop semimetals based on crystal symmetries, especially mirror symmetries, have appeared in several models[8,9,11–14] and crystal structures.[15–28]

Before the discussion of Burkov *et al.*[9], a nodal loop of a pair of coinciding Fermi rings – a nodal ring coinciding with the Fermi energy E_F – had been discovered in calculations of a ferromagnetic compensated semimetal $SrVO_3$ quantum confined within insulating $SrTiO_3$.[15] Mirror symmetry was a central feature in providing compensation and the degenerate nodal loop coinciding with E_F. What is unlikely but not statistically improbable is: (1) having the nodal loop cut by E_F while (2) the remainder of the Brillouin zone is gapped. Such loops will have real impact, and possible applications, when they are the sole bands around E_F, because they generate topological character with corresponding boundary Fermi arcs or points at zero energy.

Among his several results relating crystal symmetries to accidental degeneracies without consideration of SOC, Herring[2,3] found that inversion symmetry $\mathcal{P}$ alone is sufficient to allow nodal loops of degeneracies (fourfold: two orbitals times two spins), a result extended recently.[8,9,12] Simply stated, $\mathcal{P}$ symmetry leads to a real Bloch Hamiltonian $H(\vec{k})$ if the center of inversion is taken as the origin. The minimal (for each spin) 2×2 Hamiltonian then has the form $H(\vec{k}) = f_k\tau_x + g_k\tau_z$ (neglecting spin degeneracy for the moment) with real functions f_k, g_k; $\vec{\tau}$ represents the Pauli matrices in orbital space. Degeneracy of

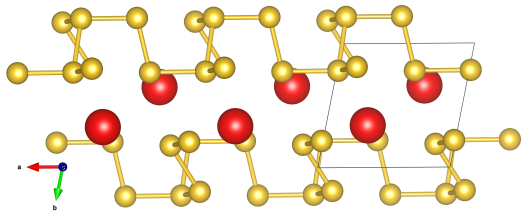

FIG. 1: Crystal structure of $CaAs_3$, viewed in the b-c plane. Arsenic atoms (yellow) form two-dimensional chains similar to black phosphorus. The center of inversion lies midway between neighboring Ca ions (shown in red).

the eigenvalues $\varepsilon_k = \pm(f_k^2 + g_k^2)^{1/2}$ requires $f_k = 0 = g_k$, two conditions on the 3D vector $\vec{k}$, giving implicitly (say) $k_y = \mathcal{K}(k_x, k_z)$ for some function $\mathcal{K}$. This condition either has no solution, or else corresponds to a loop $\mathcal{L}$ of degeneracies. Allen has given a constructive prescription[7] for following the nodal loop once a degeneracy is located.

Any such loop will not lie at a single energy,[2,7,9] and as mentioned only acquires impact when the dispersion around the loop crosses E_F, with a gap elsewhere. This intersection results in a pair (or an even number) of points where, in the absence of spin-orbit coupling, the valence and conduction band Fermi surfaces touch. The dispersion at the Fermi contact points will, barring accidents of zero probability, be massless in all three directions[3] – Weyl points. Thus at this level (before SOC) the nodal loop semimetal is a special subclass of 3D Weyl semimetal.

Topics that have not been addressed are: how little symmetry is necessary for topological character to be retained, what are the consequences, and can an example with minimum symmetry be found? The line of reasoning above applied to the case of no inversion center (*i.e.* no crystal symmetry at all) dictates that all of the coefficients of $\sigma_x, \sigma_y, \sigma_z$ in $H(\vec{k})$ vanish. Accidental point degeneracies are thus possible by tuning, while a line of degeneracies occurs with zero probability.

Discovery and study of topological nodal line semimetals protected by crystal symmetry is developing rapidly.[10,17,22,23,25] The class TPn (T=Nb, Ta; Pn=P, As) lacks an inversion center but contains several crystalline symmetries facilitating nodal loops.[18–25] The cubic antiperovskite Cu_3PdN contains nodal loops in a background of metallic bands,[12,17] the $BaTaSe_4$ family has nodal loops in its band structure enabled by symmetry, and as mentioned cubic elemental metals contain loops within their metallic bands.[10] Here we show that triclinic $CaAs_3$ is an example of a minimal symmetry nodal loop semimetal with a single loop of degeneracies, providing the "hydrogen atom" of the class of nodal semimetals..

$CaAs_3$ and three isovalent tri-arsenides (Ca→Sr, Ba, Eu) were synthesized more than thirty years ago, with their structure, transport, and optical properties studied by Bauhofer and collaborators.[29,30] $CaAs_3$ is the sole triclinic member of this family, with space group $P\bar{1}$ (#2)

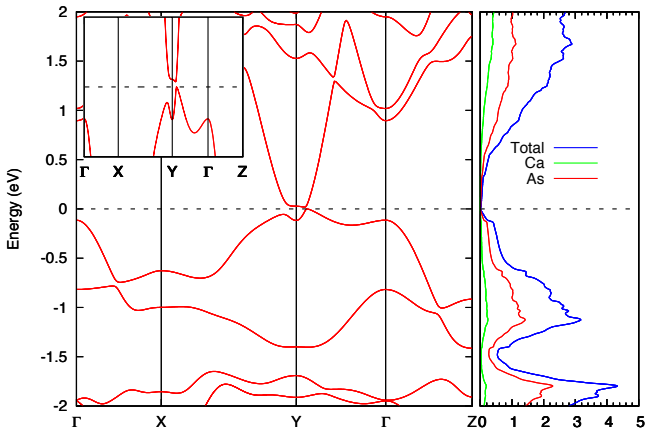

FIG. 2: Band structure of $CaAs_3$ along a few special direction, from a GGA+mBJ+SOC calculation, and (right panel) the density of states.The region of interest lies near the Y=$\vec{b}^*/2$ zone boundary (ISIM) point. Band inversion at Y can be easily imagined by ignoring the mixing that causes anticrossing along the $X-Y$ direction. Even without SOC, a gap of ~ 10 meV separates occupied and unoccupied states along the Y-Γ direction (see inset).

containing only an inversion center, lying midway between Ca sites.[29] Heavily twinned samples of $CaAs_3$ has been reported as insulating in transport measurements[29] but curiously display[30] in far infrared reflectivity a Drude weight corresponding to 10^{17}-10^{18} carriers per cm^3.

The sole symmetry condition in $P\bar{1}$ symmetry on the energy bands is $\varepsilon_{-k} = \varepsilon_k$. This simplicity indicates that "symmetry lines" are simply convenient lines with a trivial little group. $P\bar{1}$ symmetry does however provide eight inversion symmetry invariant momenta (ISIM) $m\frac{a^*}{2} + n\frac{b^*}{2} + p\frac{c^*}{2}, m, n, p = 0, 1$, in terms of the primitive reciprocal lattice vectors a^*, b^*, c^*. At these ISIMs, which are the analog of (and equivalent to) the time reversal invariant momenta (TRIMs) important in topological insulator theory,[31] eigenstates have even or odd parity. Isolated nodal loops either (a) must be centered at an ISIM, or (b) they occur in inversion related pairs. Due to the low symmetry, finding unusual characteristics (viz. the occurrence of and center of a nodal loop) necessitates meticulously searching in band inversion regions.

The linearized augmented plane wave method as implemented in WIEN2k[32] was applied with the generalized gradient approximation (GGA) exchange-correlation potential.[33] $R_m K_{max}$=7 is a sufficient cutoff for the basis function expansion in this *sp* electron material. Studies have shown that GGA may underestimate relative positioning of valence and conduction bands in semiconductors and semimetals, and that the modified Becke-Johnson (mBJ) potential provides a reasonably accurate correction.[34] Thus we rely on the GGA+mBJ combination throughout. The impact of the As SOC is assessed.

The $CaAs_3$ band structure and density of states (DOS) in directions along reciprocal lattice vectors and in the energy range from -2 eV to 2 eV, shown in Fig. 2, suggests small-gap insulating character. Valence and con-

duction bands are separated in energy except for an evident band inversion at the $Y \equiv \vec{b}^*/2$ zone boundary ISIM point. Note that with non-ISIM points having a trivial little group, bands do not cross except at accidental degeneracies, and these will coincide with any given line with zero probability.[7] The combination of $\mathcal{P}$ symmetry and periodicity is enough to ensure that band energies at $\vec{b}^*/2 \pm (0, \delta k_y, 0)$ are equal, thus (relative) band extrema occur at the ISIMs, and can be observed at X, Y, Z, and Γ in Fig. 2.

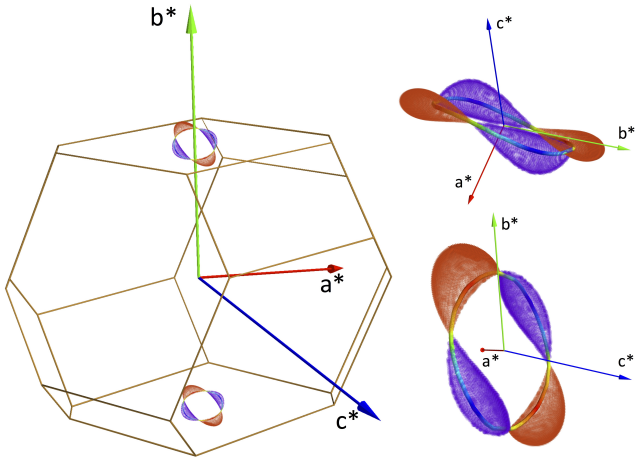

FIG. 3: Left panel: Brillouin zone of $CaAs_3$, showing the nodal loop centered at Y on the top (and bottom) face of this view of the zone. Right panels: two perspective views of the nodal line enclosed within the Fermi surfaces, with electron and hole surfaces denoted by different colors. The notations a^*, b^*, c^* of the reciprocal lattice vectors denote direction only.

Searching the band inversion region, a loop $\mathcal{L}$ of accidental degeneracies centered at Y was mapped out, *i.e.* there is no gap. Its position in the BZ is shown in Fig. 3 together with two perspective views of the Fermi surfaces (FSs). The loop, resembling a nearly planar lariat, is cut by E_F at not two but *four* points, each point being a touching point for a hole and electron FS (guaranteed by the nodal degeneracies). At this level (no SOC) the spectrum is that of a semimetal with FSs touching at four Weyl points. The loop energy lies in the -20 meV to +20 meV range, making it a very flat nodal loop in the energy domain as well as in momentum space.

The surface Fermi arcs of a few 3D Weyl semimetals are now well studied.[1] The analogous states in NLSs were discussed originally by Burkov *et al.*[9] Projected onto a surface, $\mathcal{L}$ will enclose an area (which we call a "patch") within which topologically-required surface states ("drumhead states") reside. For $CaAs_3$, $\mathcal{L}$ projected along a^* leaves a roughly circular patch, and along c^* roughly elliptical, consistent with what can be surmised from Fig. 3. The b^* axis however lies nearly within the plane of the loop, projecting to a very slender patch. A plot along a $\vec{k}$-line crossing the patch will reveal a surface band starting at the edge of this patch and ending when the k-line leaves the patch. Considering the constant energy contours (potential Fermi lines) in the patch, they may be closed lines or isolated arcs that terminate at the boundary of the patch.

Surface band plots along special directions $\bar{Y} - \bar{\Gamma} - \bar{X}$ are shown for the (001) surface in Fig. 4. As mentioned, the Fermi energy cuts the nodal loop, hence it intersects the surface patch band resulting in one or more Fermi lines on each surface. The surface band disperses along these lines shown by 70 meV. We have confirmed other studies[28,36] that indicate that surface bands obtained from Wannierization followed by truncation to obtain a surface can be sensitive to numerical procedures and the chosen surface termination, so these bands are not a definitive prediction of the physical surface states. Moreover, non-topological surface bands such as from dangling bonds may appear as well.

Effect of spin-orbit coupling. Allen demonstrated in generality the effect of SOC on the nodal loop, using a two band model in the low energy regime.[7] Without any symmetry operation to cause the SOC matrix element to vanish, which is the case in $CaAs_3$, the degeneracy is opened to a k-dependent gap ξ_k along the entire loop, which retains an inactive Kramers degeneracy. For integration around a circuit surrounding the loop $\mathcal{L}$, the topological phase $\pm\pi$ is replaced by a non-topological Berry phase that is dependent on the radius of the circuit. A magnetic field coupled to spins splits the Kramers degeneracies everywhere, giving four distinct bands near $\mathcal{L}$. Allen's paper should be consulted for specific dependencies on the materials parameters.

The SOC splitting of the atomic As $4p$ level is 270 meV. Since the bands that are inverted at Y are primarily As $4p$ character, the SOC-driven band shifts will be some appreciable fraction of this value. Given the 40 meV span in energy of the nodal loop, large enough SOC can open a gap. The bulk band projection, visible in Fig. 4, is altered little by SOC. Within the accuracy of the Wannier interpolation and surface projection, the result is characteristic of separated valence and conduction bands that however leave little or no gap.

Fig. 4 reveals that the surface spectrum evolves considerably under SOC. Most evidently, the dispersion of the valence (occupied) surface band has decreased from 70 meV to only 10 meV. If SOC coupling is large enough compared to the dispersion around $\mathcal{L}$, the system will be gapped by SOC, and $CaAs_3$ seems on the borderline of this situation. If a gap opens, it may provide a distinct topological character, signaled by the usual $\nu_0(\nu_1\nu_2\nu_3)$ indices. We calculate that $CaAs_3$, with SOC taken into account, is a topological phase with indices $\nu_0(\nu_1\nu_2\nu_3)$=1(010) using the criteria of Fu and Kane.

The spectrum in the right hand panel of Fig. 4 indicates the surface bands that will be topological insulator boundary states if SOC is large enough to give a gap. Otherwise they are topological surface states of a semimetal arising from indirect overlap, that is, a topological semimetal neither Weyl nor nodal loop. Our results in Fig. 4 indicate that $CaAs_3$ is extremely close to the topological semimetal - topological insulator transi-

tion.

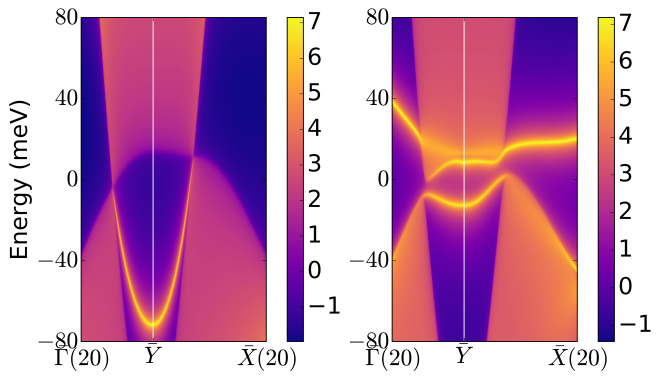

FIG. 4: Edge states (peaks in the spectral density) of $CaAs_3$ calculated using the MLWF tight binding representation truncated at the (001) surface. The panels compare spectra before (left) and after (right) inclusion of SOC. SOC hardly affects the projected bulk bands while altering the surface (bright color) bands strongly. The notation "X(20)" for example, indicates the end point is 20% of the distance toward X.

Topological nodal loop from an effective Hamiltonian. The band structure near E_F of $CaAs_3$, with the highest valence band inverted across the lowest conduction band at Y, was fit to a tight-binding model. Away from Y $CaAs_3$ is gapped, making this compound ideal for observing a topological nodal line. For simplicity one can imagine the crystal deformed by an affine transformation to have orthogonal axes with a=b=c=1. We consider the following two orbital, non-inversion symmetric Hamiltonian which reproduces the essential features of the inverted band region of $CaAs_3$. It includes nearest neighbor hopping between like orbitals $\{t_\alpha, \alpha = 1-3\}$, and between unlike orbitals $\{t_\alpha, \alpha = 4-6\}$ having differing parity:

$$\begin{aligned} \tilde{H}(\vec{k}) &= g_{\vec{k}}\tau_z + f_{\vec{k}}\tau_x + i\xi\sigma_z\tau_x \\ f(k_a,k_b,k_c) &= t_4 \sin k_a + t_5 \sin k_b + t_6 \sin k_c \\ g(k_a,k_b,k_c) &= m - t_1\cos k_a - t_2 \cos k_b - t_3 \cos k_c, \end{aligned}$$

where $\{\tau_j\}$,$\{\sigma_j\}$ are the 2×2 matrices in orbital and spin space respectively, and ξ is the SOC parameter. This Hamiltonian describes two particle-hole symmetric bands $\pm|g_k|$ with centers separated by $2|m|$, coupled by f_k, and including intra-orbital SOC, with eigenenergies $\varepsilon_{k,\pm} = \pm\sqrt{g_{\vec{k}}^2 + f_{\vec{k}}^2 + \xi^2}$. Evidently SOC ($\xi \neq 0$) splits the degeneracy everywhere.[7,8] To mimic $CaAs_3$ we consider the site energy m and hopping parameters (in eV) $m = 1.64$, $t_1 = 0.37$, $t_2 = -0.95$, $t_3 = 0.37$, $t_4 = -0.18$, $t_5 = 0.12$, $t_6 = 0.38$. Without SOC ($\xi = 0$), degeneracy $f_k = 0 = g_k$ is realized around a nodal loop flat in energy (at zero energy). The loop, centered at Y but otherwise depending on parameters, and shown in the left panel of Fig. 5, resembles the nodal loop of $CaAs_3$ pictured in Fig. 3.

The evolution of the loop topology can be followed by varying the band separation $2m$. Two types of lines of accidental degeneracies may emerge from the Hamiltonian: a closed nodal loop as in $CaAs_3$, or a line extending from zone to zone, which by zone periodicity become closed lines on the 3D-torus, the difference from the former being that they must occur in pairs. In Fig. 5, the two types of loops are plotted in the first Brillouin zone. On the left, where m=1.44, a single loop is centered at Y.

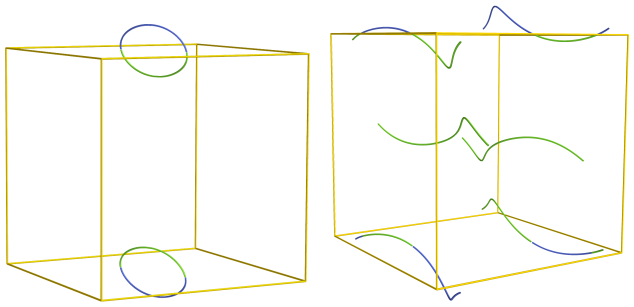

FIG. 5: Nodal lines of accidental degeneracies for the model Hamiltonian' the dots indicate where a loop passes into a neighboring Brillouin zone. For m=1.44 on the left, a single loop is centered on the ISIM point $\frac{\vec{b}^*}{2}$. The m=0 case is shown on the right, with two pairs of inversion symmetry related lines threading from zone to zone.

Varying m tunes the system through an evolution from an odd number (one) to an even number (four) of nodal loops. The right panel in Fig. 5 (m=0) has two pairs of inversion symmetric nodal loops threading through extended Brillouin zones. Because the loop is flat in energy (at zero), adding SOC immediately opens a global gap of 2ξ. We find the resulting state to have indices 0(000), *i.e.* a trivial insulator, A different, lower symmetry model would be necessary to produce a topological insulating state such as occurs in 1(010) $CaAs_3$.

In this work we have studied the electronic and topological properties of triclinic $CaAs_3$, which is distinguished by possessing the lowest possible symmetry for a nodal loop semimetal. In the absence of spin-orbit coupling, $CaAs_3$ has a single nodal loop (others have loops occurring in pairs) that is cut by the Fermi level four times. Spin-orbit coupling leads not only to lifting of the nodal loop degeneracies and separation of valence and conduction bands complexes. An effective Hamiltonian demonstrates that a variety of types and numbers of nodal loops will emerge as parameters are varied. This model provides guidance for engineering topological transitions in $CaAs_3$ and related materials by applying external tensile or compressive strains, or by alloying with isovalent atoms on either site.

We have benefited from comments on the manuscript from A. Essin, from discussions of topological aspects with K. Koepernik and J. Kŭnes, and from T. Siegrist and A. P. Ramirez on $CaAs_3$ samples and transport data. The calculations used high performance clusters at the National Supercomputer Center in Guangzhou, and resources of the National Energy Research Scientific Computing Center (NERSC), a DOE Office of Science User Facility supported by the Office of Science of the U.S.

Department of Energy under Contract No. DE-AC02-05CH11231.. W.E.P. was supported by the NSF grant DMR-1534719 under the program *Designing Materials to Revolutionize and Engineer our Future*. Z.P.Y. acknowledges support from Fund 310432102 of Beijing Normal University and Chinese National Youth Thousand Talent grant 370221001. Y.Q. acknowledges support from Beijing Normal University.

[1] See, for example, X. Wan, A. M. Turner, A. Vishwanath, and S. Y. Savrasov, Topological semimetal and Fermi-arc surface states in the electronic structure of pyrochlore iridates, Phys. Rev. B **83**, 205101 (2011).

[2] W. C. Herring, Accidental Degeneracy in the Energy Bands of Crystals, Phys. Rev. **52**, 365 (1937).

[3] W. C. Herring, On energy coincidences in the theory of Brillouin zones (Lancaster Press, Lancaster, PA, 1937). PhD thesis.

[4] J. von Neumann and E. P. Wigner, On the behavior of eigenvalues in adiabatic processes, Physik. Z. **30**, 467 (1929). Translated in R. S. Knox and A. Gold, *Symmetry in the Solid State* (Benjamin, New York, 1964), p. 167.

[5] E. I. Blount, in *Solid State Physics*, eds. F. Seitz and D. Turnbull (Academic Press, New York, 1962), vol 13, p. 306.

[6] M. V. Berry, Aspects of degeneracy, in *Chaotic Behavior in Quantum Systems*, ed. G. Casatil (Plenum, New York, 1985), pp. 123-140.

[7] P. B. Allen, What happens to geometric phase when spin-orbit interactions lift band degeneracies? arXiv:0709.1457 (2007).

[8] C. Fang, Y. Chen, H.-Y. Kee, and L. Fu, Topological nodal line semimetals with and without spin-orbital coupling, Phys. Rev. B **92**, 081201 (2015).

[9] A. A. Burkov, M. D. Hook, and L. Balents, Topological nodal semimetals, Phys. Rev. B **84**, 235126 (2011).

[10] M. Hirayama, R. Okugawa, T. Miyake, and S. Murakami, Topological Dirac nodal lines in fcc calcium, strontium, and ytterbium, arXiv:1602.06501.

[11] M. Phillips and V. Ali, Tunable line node semimetals, Phys. Rev. B **90**, 115111 (2014).

[12] Y. Kim, B. J. Wieder, C. L. Kane, and A. M. Rappe, Dirac line nodes in inversion-symmetric crystals, Phys. Rev. Lett. **115**, 036806 (2015).

[13] T. T. Heikkilä and G. E. Volovik, Nexus and Dirac lines in topological materials, New J. Phys. **17**, 093019 (2015).

[14] K. Mullen, B. Uchoa, and D. T. Glatzhofer, Line of Dirac Nodes in Hyperhoneycomb Lattices, Phys. Rev. Lett. **115**, 026403 (2015).

[15] V. Pardo and W. E. Pickett, Electron Confinement, Orbital Ordering, and Orbital Moments in $d^0 - d^1$ Oxide Heterostructures, Phys. Rev. B **81**, 245117 (2010)

[16] C. Fang, M. J. Gilbert, X. Dai, and B. A. Bernivig, Multi-Weyl topological semimetals stabilized by point group symmetry, Phys. Rev. Lett. **108**, 266802 (2012).

[17] R. Yu, H. Weng, Z. Fang, X. Dai, and X. Hu, Topological Node-Line Semimetal and Dirac Semimetal State in Antiperovskite Cu_3PdN, Phys. Rev. Lett. **115**, 036807 (2015).

[18] S.-M. Huang *et al.*, A Weyl fermion semimetal with surface Fermi arcs in the transition metal monopnictide TaAs class, Nat. Commun. **6**, 1 (2015).

[19] D.-F. Xu, Y.-P. Du, Z. Wang, Y.-P. Li, X.-H. Niu, Q. Yao, P. Dudin, Z.-A. Xu, X.-G. Wan, and D.-L. Feng, Chin. Phys. Lett. **32**, 107101 (2015).

[20] B. Q. Lv *et al.*, Observation of Weyl nodes in TaAs, Nature Physics **11**, 724-727 (2015).

[21] C. Shekhar *et al.*, Extremely large magnetoresistance and ultrahigh mobility in the topological Weyl semimetal candidate NbP, Nat. Phys. **11**, 645 (2015).

[22] H. Weng, C. Fang, Z. Fang, B. A. Berniveg, and X. Dai, Weyl semimetal phase in noncentrosymmetric transition-metal monophosphides, Phys. Rev. X **5**, 011029 (2015).

[23] K.-H. Ahn, K.-W. Lee, and W. E. Pickett, Spin-orbit driven interaction collective electron-hole excitations in a noncentrosymetric nodal loop Weyl semimetal, Phys. Rev. B **92**, 115149 (2015).

[24] Y. Sun, S.-C. Wu, and B. Yan, Topological surface states and Fermi arcs of the noncentrosymmetric Weyl semimetals TaAs, TaP, NbAs, and NbP, arxiv:1508.06649.

[25] L. X. Yang, Z. K. Liu, Y. Sun, H. Peng, H. F. Yang, T. Zhang, B. Zhou, Y. Zhang, Y. F. Guo, M. Rahn, D. Prabhakaran, Z. Hussain, S.-K. Mo, C. Felser,B. Yan, and Y. L. Chen, Weyl semimetal phase in the non-centrosymmetric compound TaAs, Nat. Phys. **11**, 728 (2015).

[26] M. Neupane *et al.*, Observation of topological nodal fermion semimetal phase in ZrSiS, Phys. Rev. B **93**, 195106 (2016).

[27] H. Huang, J. Liu, D. Vanderbilt, and W. Duan, Topological nodal-line semimetals in alkaline-earth stannides, germanides, and silicides, Phys. Rev. B **93**, 201114 (2016).

[28] J. Zhao, R. Yu, H. Weng, and Z. Fang, Topological node-line semimetal in compressed balck phosphorus, arXiv:1511.05704.

[29] W. Bauhofer, M. Wittmann and H. G. v. Schnering, Structure, electrical and magnetic properties of $CaAs_3$, $SrAs_3$, $BaAs_3$, and EuP_3, J. Phys. Chem. Solids, **42**, 687 (1981).

[30] B. Oleš and H. G. von Schnering, Infrared studies of phonons and free carriers in $CaAs_3$, $SrAs_3$, $BaAs_3$, and α-EuP_3, J. Phys. C **14**, 5559 (1981).

[31] J. C. Y. Teo, L. Fu, and C. L. Kane, Surface states and topological invariants in three-dimensional topological insulators: Application to $Bi_{1x}Sb_x$, Phys. Rev. B **78**, 045426 (2008).

[32] P. Blaha, K. Schwarz, G. Madsen, D. Kvasnicka and J. Luitz, WIEN2k, An Augmented Plane Wave + Local Orbitals Program for Calculating Crystal Properties (Karlheinz Schwarz, Techn. Universität Wien, Austria), 2001. ISBN 3-9501031-1-2

[33] J. P. Perdew, K. Burke and M. Ernzerhof, Generalized Gradient Approximation Made Simple, Phys. Rev. Lett. **77**, 3865 (1996).

[34] H. Zhang and S.-C. Zhang, Topological insulators from the perspective of first-principles calcuulations, Phys. Status Solidi (RRL) **7** 1862-6270 (2013)

[35] H. Weng, Y. Liang, Q. Xu, R. Yu, Z. Fang, X. Dai, and Y. Kawazoe, Topological node-line semimetal in three-dimensional graphene networks, Phys. Rev. B **92**, 045108 (2015).

[36] S. T. Pi, H. Wang, J. Kim, R. Wu, Y.-K. Wang, and C.-K. Lu, Design of a giant-gap 3D topological insulator: the case of double perovskites, arXiv:1609.09204.